OPEN ACCESS
IOP Publishing
Journal of Physics A: Mathematical and Theoretical
J. Phys. A: Math. Theor. **56** (2023) 025003 (11pp)
https://doi.org/10.1088/1751-8121/acb1e0

Dual unitary circuits in random geometries

Yusuf Kasim* **and Tomaž Prosen**

Department of Physics, Faculty of Mathematics and Physics, University of Ljubljana, SI-1000 Ljubljana, Slovenia

E-mail: yusuf.kasim@fmf.uni-lj.si

Received 24 June 2022; revised 22 December 2022
Accepted for publication 10 January 2023
Published 30 January 2023

Abstract

Recently introduced dual unitary brickwork circuits have been recognised as paradigmatic exactly solvable quantum chaotic many-body systems with tunable degree of ergodicity and mixing. Here we show that regularity of the circuit lattice is not crucial for exact solvability. We consider a circuit where random 2-qubit dual unitary gates sit at intersections of random arrangements of straight lines in two dimensions (*mikado*) and analytically compute the variance of the spatio-temporal correlation function of local operators. Note that the average correlator vanishes due to local Haar randomness of the gates. The result can be physically motivated for two random mikado settings. The first corresponds to the thermal state of free particles carrying internal qubit degrees of freedom which experience interaction at kinematic crossings, while the second represents rotationally symmetric (random euclidean) space-time.

Keywords: random geometry, statistical physics, quantum circuits, dual unitarity

(Some figures may appear in colour only in the online journal)

1. Introduction

Taming real time dynamics of interacting many-body systems represents one of the main challenges of theoretical physics. The cleanest and most versatile setting to study interacting many-body dynamics is arguably that of quantum circuits with up to 2-qubit gates (representing local interactions). Although the classical simulation of generic quantum circuits has been in general

* Author to whom any correspondence should be addressed.

recognised as intractable, and is currently employed to demonstrate the so-called supremacy of quantum computers [1], we have recently identified an interesting type of so-called dual unitary circuits where the problem of computing certain dynamical quantities, such as two-point spatio-temporal correlation functions [2–7], quantum quenches [8], spectral form factors [9, 10], operator entanglement [11], etc, can be solved efficiently or even analytically. Dual unitary circuits, with the gates arranged on a regular brickwork pattern, possess a unique defining feature: specifically, the many-body propagator is not only unitary in the time direction, but can also be identified with a unitary dynamics in the space direction. Furthermore, one can argue that chaotic variants of dual unitary circuits, with provable random matrix level statistics and exponentially decaying temporal correlations, represent an exactly solvable instance of ergodic and mixing quantum many-body dynamics. As such, unlike integrable systems, they may be expected to be structurally stable against small perturbations breaking dual-unitarity [12].

Dual unitary circuits studied so far were all defined on regular lattices, either with 2-on-2 gates arranged as vertices of a square lattice (brickwork), or with 3-on-3 gates arranged as vertices of a hexagonal lattice [13]. By factorising these so-called tri-unitary 3-on-3 gate in terms of triples of dual unitary 2-on-2 gates, the latter can in fact be represented as the circuit on the Kagome lattice where 2-qubit dual unitary gates are placed on all intersections of pairs of lines.

In this paper, we propose an additional conceptual modification towards a definition of more general dual unitary systems in 1+1 dimensions. Instead of insisting on a regular pattern of 2-on-2 dual unitary gates, we consider an arbitrary arrangement of straight lines in 1+1 dimensions (mikado). Stipulating that each line (wire) carries a qubit state, we place a (possibly different) dual unitary gate U, with 4×4 matrix U^{kl}_{ij} $(i,j,k,l\in\{1,2\})$ at any intersection. Requirement of dual-unitarity of U, means that both U^{kl}_{ij} and $\tilde{U}^{kl}_{ij}=U^{jl}_{ik}$ should be unitary. Assuming that none of the lines (wires) is precisely parallel to the time axis $t=\text{const}$, we thus define a circuit dynamics between times $t=0$ and $t=T$, where the size of the system N—the number of qubits—is equal to the total number of lines (figure 1(a)). By requirement of dual-unitarity, such circuit is unitary, irrespective of the orientation of each gate, i.e. which pair of adjacent lines are considered as input/output qubits. Requiring gates' unitarity alone, the circuit generally possesses a unique (fixed) direction of time and reduces to the so-called hybrid semiclassical model of [14], where qubit/spin degrees of freedom pairwise interact when classical free-particle trajectories cross.

2. Mikado dual unitary circuits

We investigate the behavior of spatio-temporal correlation functions and their decay using random dual unitary gates in random geometries, with an example shown in figure 1(a). Let us write the full unitary circuit between times t_1 and t_2 for a fixed mikado arrangement as $\mathbb{U}(t_1,t_2)\in\mathrm{End}((\mathbb{C}^2)^{\otimes N})$. Denoting the nth line coordinate at time t as $x_n(t)$, we define the kth moment of spatiotemporal correlator between a pair of local operators $a,b\in\mathrm{End}(\mathbb{C}^2)$, with local embeddings $a_n,b_n\in\mathrm{End}((\mathbb{C}^2)^{\otimes N})$, as

$$C^{(k)}_{ab}(x_{\mathrm{i}},t_{\mathrm{i}};x_{\mathrm{f}},t_{\mathrm{f}})=\sum_{n,n'}\delta(x_{\mathrm{i}}-x_n(t_{\mathrm{i}}))\delta(x_{\mathrm{f}}-x_{n'}(t_{\mathrm{f}}))\times\left\{2^{-N}\mathrm{tr}\left(a_n\mathbb{U}(t_1,t_2)^{\dagger}b_{n'}\,\mathbb{U}(t_1,t_2)\right)\right\}^k. \tag{1}$$

In the next step we use the folded picture [15] (following the notation of [7, 12]), to rewrite (1) as

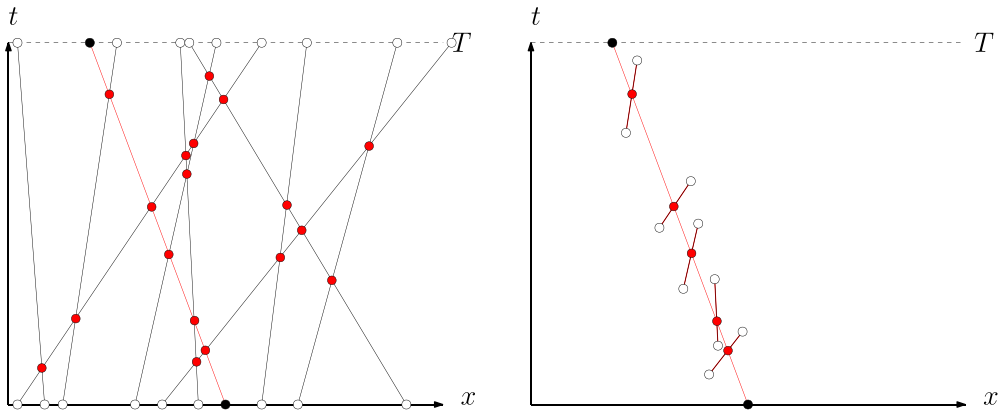

(a) Before contraction (b) After contraction

Figure 1. Example of a local correlation function of a dual unitary random mikado lattice (a). The crossings between wires (red circles) represent dual-unitary gates, while the full circles (bullet) at the initial and final time represent the initial and final local operator. The panel on the right (b) shows the identical tensor network obtained after implementing all dual unitarity conditions (contractions). The correlator is nonzero only if initial and final operator are connected by a straight wire (red line).

$$C^{(k)}_{ab}(x_1,t_1;x_2,t_2)=\sum_{n,n'}\delta(x_1-x_n(t_1))\delta(x_2-x_{n'}(t_2))\langle a_n|\mathbb{W}(t_1,t_2)|b_{n'}\rangle^k. \qquad (2)$$

Here $\mathbb{W}(t_1,t_2)\in\mathrm{End}((\mathbb{C}^4)^{\otimes N})$ is exactly the same unitary circuit as $\mathbb{U}(t_1,t_2)$ but generated by the folded 2-qudit (operator) gates with $d=4$, for which we will use a diagrammatic representation

$$W^{(kk')(ll')}_{(ii')(jj')}=U^{kl}_{ij}\bar{U}^{k'l'}_{i'j'}=$$

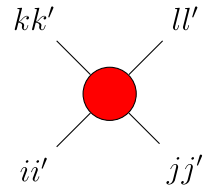

. (3)

The wires thus carry local operator-states, which we will graphically designate by •. The self-contraction of the wire (summation over unprimed/bra and primed/ket indices in equation (3)) either represents a unit operator or taking the trace and shall be designated by ∘.

The property of dual unitarity can then be neatly expressed as a single diagram, stating that any pair of self-contracting wires can be simply pulled thru the interaction vertex (note that a pair of 'operator wires' can have a pair of contraction symbols ∘ on any side):

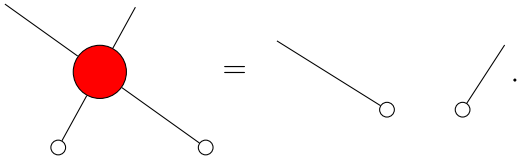

. (4)

Dual unitary gates of qubits can be completely parametrised as [2]:

$$U = e^{i\phi}(u_+ \otimes u_-)V[J](v_- \otimes v_+)$$
$$V[J] = \exp\left[-i\left(\frac{\pi}{4}\sigma^x \otimes \sigma^x + \frac{\pi}{4}\sigma^y \otimes \sigma^y + J\sigma^z \otimes \sigma^z\right)\right], \tag{5}$$

where $\sigma^{x,y,z}$ are the Pauli matrices, $u_\pm, v_\pm \in \mathrm{SU}(2)$ are arbitrary local 1-qubit gates, and $J \in [0, \frac{\pi}{4}]$ is an interaction parameter which uniquely determines the entangling power of the gate [5]. For instance, $J = \pi/4$ corresponds to the non-interacting (SWAP) gate, while a region around $J = 0$ yields the case of the *maximal chaos* [11].

Diagram equation (4) can be used to drastically simplify the circuit of figure 1(a). Assuming that the operators a, b are traceless, the diagram of figure 1(a) contracts to zero, unless we place the operators a, b on the same line/wire. In the latter case, the correlator reduces to the product of unital 1-qubit quantum channels, as depicted in figure 1(b). These local unital channels, written in the 3-dimensional Pauli basis $\{\sigma^\alpha; \alpha = x, y, z\}$—while on the unit operator $\mathbb{1}$ they act trivially—are represented with elementary diagrams

$$\mathcal{M}[u, v] = R[u]\, D\, R[v] =$$

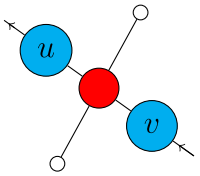

. (6)

Here, $R[w]$ is the adjoint, 3-dimensional representation of $w \in \mathrm{SU}(2)$ and

$$D = \begin{pmatrix} \sin 2J & 0 & 0 \\ 0 & \sin 2J & 0 \\ 0 & 0 & 1 \end{pmatrix}. \tag{7}$$

Therefore, the kth moment of the correlation function for a fixed mikado arrangement reads

$$C^{(k)}_{ab}(x_\mathrm{i}, t_\mathrm{i}; x_\mathrm{f}, t_\mathrm{f}) = \sum_n \delta(x_\mathrm{i} - x_n(t_\mathrm{i}))\delta(x_\mathrm{f} - x_n(t_\mathrm{f})) \times \langle a|\mathcal{M}[u_m, v_m] \cdots \mathcal{M}[u_2, v_2]\mathcal{M}[u_1, v_1]|b\rangle^k, \tag{8}$$

where $\langle a|, |b\rangle$ are 3-dimensional vectors representing operators a, b in the Pauli basis, while u_j, and v_j, $j = 1, \ldots, m$ are SU(2) 1-qubit gates before, and after, the interaction vertices (in parametrization (5)) along all $m = m(n)$ intersections of the line/wire n with all the other lines between times t_i and t_f.

Finally, we write the average moment of spatio-temporal correlator as an expectation value over random mikado arrangements and Haar random gates u_j, v_j, while the interaction parameter J is kept fixed as the key parameter (coupling constant) of the model:

$$\mathcal{C}^{(k)}_{ab}(x, t) = \mathbb{E}\left(C^{(k)}_{ab}(0, 0; x, t)\right) = \frac{1}{t} p\left(\frac{x}{t}\right) \sum_{m=0}^{\infty} \mathbb{P}(m|x, t)\mathcal{C}^{(k)}_{ab}(m). \tag{9}$$

In random mikado arrangements we assume translational invariance in x and t, hence $N = \infty$, so we can fix $x_\mathrm{i} = 0$, $t_\mathrm{i} = 0$. $p(v)$ denotes the probability density that a randomly chosen line (n) has the velocity/slope $v_n = v$, while $\mathbb{P}(m|x, t)$ denotes the probability that a line section from $(0, 0)$ to (x, t) has exactly m crossings with other lines, while $C^{(k)}_{ab}(m)$ denotes an average over Haar random u_j, v_j:

$$\mathcal{C}^{(k)}_{ab}(m) = \mathbb{E}\left(\langle a|\mathcal{M}[u_m, v_m] \cdots \mathcal{M}[u_2, v_2]\mathcal{M}[u_1, v_1]|b\rangle^k\right). \tag{10}$$

We can evaluate the expectation (10) by using k replicas and explicit Haar measure for integration over Euler angle parametrization of the rotation matrix $R[u] \equiv R(\vec{\theta}) \equiv R(\theta_1, \theta_2, \theta_3)$,

$$R(\theta_1,\theta_2,\theta_3) = \begin{pmatrix} \cos\theta_1 & -\sin\theta_1 & 0 \\ \sin\theta_1 & \cos\theta_1 & 0 \\ 0 & 0 & 1 \end{pmatrix} \begin{pmatrix} 1 & 0 & 0 \\ 0 & \cos\theta_2 & -\sin\theta_2 \\ 0 & \sin\theta_2 & \cos\theta_2 \end{pmatrix} \begin{pmatrix} \cos\theta_3 & -\sin\theta_3 & 0 \\ \sin\theta_3 & \cos\theta_3 & 0 \\ 0 & 0 & 1 \end{pmatrix} \tag{11}$$

$$\int \mathrm{d}\mu(\vec{\theta}) = \frac{1}{8\pi^2} \int_0^{2\pi} \mathrm{d}\theta_1 \int_0^{\pi} \mathrm{d}\theta_2 \int_0^{2\pi} \mathrm{d}\theta_3 \sin(\theta_2). \tag{12}$$

Specifically,

$$\begin{aligned} \mathcal{C}_{ab}^{(k)}(m) &= \langle a|^{\otimes k} \int \overleftarrow{\prod_{1\leqslant j\leqslant m}} \mathrm{d}\mu(\vec{\theta}_j)\mathrm{d}\mu(\vec{\theta}_j')R(\vec{\theta}_j)^{\otimes k} D^{\otimes k} R(\vec{\theta}_j')^{\otimes k} |b\rangle^{\otimes k} \\ &= \langle a|^{\otimes k} \mathcal{T}^m |b\rangle^{\otimes k}, \end{aligned} \tag{13}$$

where $\mathcal{T}$ is the $3^k \times 3^k$ transfer matrix

$$\mathcal{T} = \mathcal{P} D^{\otimes k} \mathcal{P}, \quad \mathcal{P} := 3^{-k/2} \int \mathrm{d}\mu(\vec{\theta}) R(\vec{\theta})^{\otimes k}. \tag{14}$$

While the projector $\mathcal{P}$ can be in general expressed in terms of the Weingarten functions [16, 17], the results for the first and the second moment can be obtained fully explicitly.

Let us assume that a, b is an arbitrary pair of traceless and Hilbert-Schmidt normalized observables, $\mathrm{tr}a = \mathrm{tr}b = 0$, $\mathrm{tr}a^2 = \mathrm{tr}b^2 = 1$.

For $k = 1$, we find $\mathcal{P} = 0$, and hence the average (mean) correlator vanishes for any $m > 0$,

$$\mathcal{C}_{ab}^{(1)}(m) = \delta_{m,0}. \tag{15}$$

For $k = 2$, we find that

$$\mathcal{P} = \frac{1}{3} \begin{pmatrix} 1 & 0 & 0 & 0 & 1 & 0 & 0 & 0 & 1 \\ 0 & 0 & 0 & 0 & 0 & 0 & 0 & 0 & 0 \\ 0 & 0 & 0 & 0 & 0 & 0 & 0 & 0 & 0 \\ 0 & 0 & 0 & 0 & 0 & 0 & 0 & 0 & 0 \\ 1 & 0 & 0 & 0 & 1 & 0 & 0 & 0 & 1 \\ 0 & 0 & 0 & 0 & 0 & 0 & 0 & 0 & 0 \\ 0 & 0 & 0 & 0 & 0 & 0 & 0 & 0 & 0 \\ 0 & 0 & 0 & 0 & 0 & 0 & 0 & 0 & 0 \\ 1 & 0 & 0 & 0 & 1 & 0 & 0 & 0 & 1 \end{pmatrix}, \tag{16}$$

and the transfer matrix has rank one

$$\mathcal{T} = \lambda |\Psi\rangle\langle\Psi|, \quad \lambda = \frac{1}{3}(2 - \cos 4J), \quad |\Psi\rangle = \frac{1}{\sqrt{3}} \sum_{\alpha=1}^{3} |\alpha\rangle \otimes |\alpha\rangle. \tag{17}$$

Hence the second moment of the correlator reads

$$\mathcal{C}_{ab}^{(2)}(m) = \delta_{m,0} + (1 - \delta_{m,0}) \frac{1}{3} \lambda^m = \delta_{m,0} + (1 - \delta_{m,0}) \frac{1}{3^{m+1}} (2 - \cos(4J))^m, \tag{18}$$

while the variance is given by:

$$\mathcal{C}_{ab}^{[2]}(m) = \mathcal{C}_{ab}^{(2)}(m) - \left(\mathcal{C}_{ab}^{(1)}(m)\right)^2 = (1 - \delta_{m,0}) \frac{1}{3^{m+1}} (2 - \cos(4J))^m. \tag{19}$$

3. Two settings of random mikado networks

In this section, we will introduce the two settings of random networks that we studied (see figure 2). In the first setting, studied in section 3.1, we assume to have a gas of $N \to \infty$ identical free non-interacting classical point particles in thermal equilibrium, at fixed temperature and density. We then assume that particles carry internal quantum degrees of freedom—qubits, which interact via random dual unitary gate whenever two particles meet (and their trajectories cross).

In the second setting, studied in section 3.2, we consider a rotationally and translationally invariant random arrangement of wires, such that intersections with any, arbitrarily oriented fixed line have a constant density.

Distinct outputs of these settings are conditional number-of-crossed-wires probabilities $\mathbb{P}(m|x,t)$ which is the essential input into the formula (9).

3.1. Thermal distribution of wires

Here we consider a gas of $N \to \infty$ non-interacting particles with coordinates $x_n(t) = x_n + v_n t$. We assume the gas to be in thermal equilibrium, with mean interparticle spacing $a = 1$ (or density one), setting the length scale, and inverse temperature $\beta = 1$, setting the time scale. This means that coordinates of particles $x_n(t)$ form a Poisson point process on $\mathbb{R}$ with mean spacing $a = 1$ for all times t, and that velocities v_n are i.i.d. normal Gaussian variables with zero mean and unit variance

$$p(v) = \frac{1}{\sqrt{2\pi}} e^{-v^2/2}. \tag{20}$$

Given a random line $x_n(t)$, $t \in [0,T]$, we shall now write the probability distribution $\mathbb{P}(m|X,T)$, where $X = v_n T$, of the number m of other lines $x_{n'}(t)$ crossing the line n during the time $t \in [0,T]$. As the wires are statistically independent, the distribution is clearly the Poissonian

$$\mathbb{P}(m|X,T) = \frac{[\bar{m}(X,T)]^m e^{-\bar{m}(X,T)}}{m!}. \tag{21}$$

We shall now derive the average number of crossings $\bar{m}(X,T)$.

We first write the probability of crossing of a pair of randomly chosen wires, indicated as $n = 0$ and $n = 1$, for $t \in [0,T]$. For convenience, we choose the reference initial coordinate at the origin $x_0 = 0$, and the second one at $x_1 = x$, with slopes/velocities, v_0, v_1, respectively. The condition for crossing in the targeted time interval then reads $0 < x/(v_0 - v_1) < T$, which gives the probability, after integrating over the normally distributed velocity v_1

$$\begin{aligned}\mathbb{P}(v_0,x,T) &= \frac{1}{\sqrt{2\pi}} \left(\int_{-\infty}^{x/T - v_0} e^{-\frac{1}{2}v_1^2} + \int_{x/T-v_0}^{\infty} e^{-\frac{1}{2}v_1^2} \right) \mathrm{d}v_1 \\ &= \frac{1}{2} + \frac{\mathrm{sgn}(x)}{2} \mathrm{erf}\left(\frac{1}{\sqrt{2}} \left(v_0 - \frac{x}{T} \right) \right). \end{aligned} \tag{22}$$

As the initial coordinates x of the wires are distributed uniformly randomly on $\mathbb{R}$ with density one, the average number of crossings then reads (noting $v_0 = X/T$):

$$\bar{m}(X,T) = \int_{-\infty}^{\infty} \mathrm{d}x \mathbb{P}\left(\frac{X}{T}, x, T \right) = \sqrt{\frac{2}{\pi}} T \exp\left(-\frac{X^2}{2T^2} \right) + X \mathrm{erf}\left(\frac{X}{\sqrt{2}T} \right). \tag{23}$$

3.2. Isotropic distribution of wires

In the second setting, we assume that the wire distribution is isotropic and translationally invariant, with density one. This immediately implies that the slope (velocity) distribution is given by a distribution of a tangent of a uniformly distributed angle

$$p(v) = \frac{1}{\pi(1+v^2)}, \tag{24}$$

while the distribution of the number of crossings is again Poissonian (21), with the average that is given by the length of line-section (wire)

$$\bar{m}(X,T) = \sqrt{X^2+T^2}. \tag{25}$$

4. The variance of spatio-temporal correlation function

Finally, we collect the pieces ((9), (19) and (21)) together, and write the final result for the variance of local two-point correlation function in mikado dual unitary circuits:

$$\begin{aligned}\mathcal{C}^{[2]}_{ab}(X,T) &= \frac{1}{T}p\left(\frac{X}{T}\right)\sum_{m=0}^{\infty}(1-\delta_{m,0)})\frac{1}{3^{m+1}}\frac{[\bar{m}(X,T)]^m e^{-\bar{m}(X,T)}}{m!}(2-\cos 4J)^m \\ &= \frac{1}{3T}p\left(\frac{X}{T}\right)\sum_{m=1}^{\infty}\frac{[\bar{m}(X,T)]^m e^{-\bar{m}(X,T)}}{m!}\left(1-\frac{2}{3}\cos^2(2J)\right)^m \\ &= \frac{1}{3T}p\left(\frac{X}{T}\right)\left\{\exp\left(-\frac{2}{3}\cos^2(2J)\bar{m}(X,T)\right)-\exp\left(-\bar{m}(X,T)\right)\right\}. \end{aligned} \tag{26}$$

For the two different distributions of random mikados that we have studied in section 3 we can write the result even more explicitly:

(a) For the thermal case, we use ((20) and (23)) and find

$$\begin{aligned}\mathcal{C}^{[2]}_{ab}(X,T) = \frac{1}{3\sqrt{2\pi}T}\exp\left(-\frac{X^2}{2T^2}\right)\left\{\exp\left[-\frac{2\cos^2 2J}{3}\left\{\sqrt{\frac{2}{\pi}}Te^{-\frac{X^2}{2T^2}}+X\mathrm{erf}\left(\frac{X}{\sqrt{2}T}\right)\right\}\right]\right. \\ \left.-\exp\left[-\sqrt{\frac{2}{\pi}}Te^{-\frac{X^2}{2T^2}}-X\mathrm{erf}\left(\frac{X}{\sqrt{2}T}\right)\right]\right\}\end{aligned} \tag{27}$$

(b) For the isotropic case, the result is even simpler via (24) and (25)

$$\mathcal{C}^{[2]}_{ab}(X,T) = \frac{T}{3\pi(X^2+T^2)}\left\{\exp\left(-\frac{2\cos^2 2J}{3}\sqrt{X^2+T^2}\right)-\exp\left(-\sqrt{X^2+T^2}\right)\right\}. \tag{28}$$

For illustration, we show in figure 3 the variance of the correlator for an exemplar value of the interaction parameter $J=\pi/4-1/2$. Specifically, figure 3(a) depicts the correlator in the thermal case (equation (27)), and figure 3(b) in the isotropic case (equation (28)).

Equation (26) shows that there are two exponential terms contributing to the decay of the variance of the correlation functions. The first term $\exp(-2/3\cos^2(2J)\bar{m}(X,T))$ and the second $\exp(-\bar{m}(X,T))$. The interaction parameter J contributes only to the first term, while the terms with $\bar{m}$ come from the geometry and are independent of J. It is clear to see that for $J=0$ the decay will be maximal, while as $J\to\pi/4$ the interaction term contribution becomes smaller and the decay is governed by the geometry.

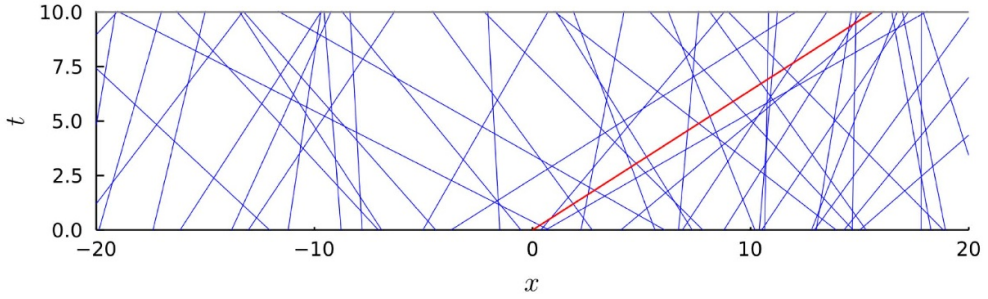

(a) Example of a realization of a mikado circuit for the case of thermal distribution of slopes.

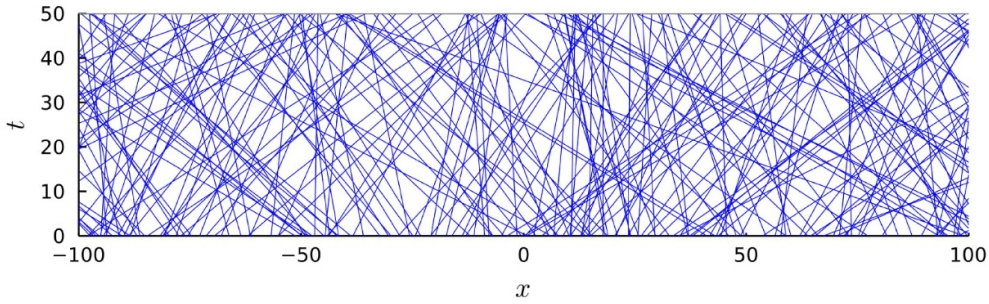

(b) Zoom out of the thermal case.

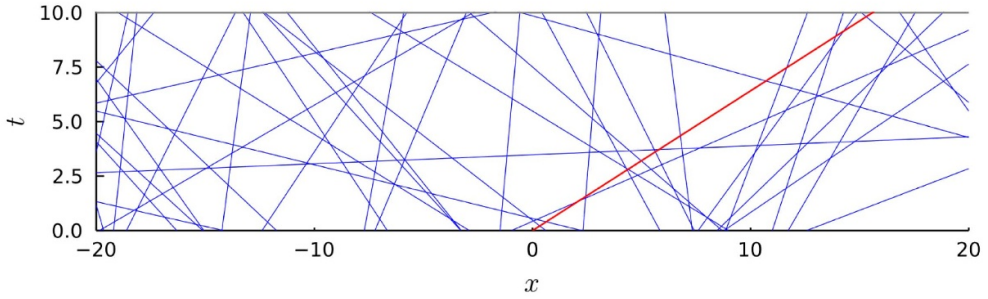

(c) Example of a realization of a mikado circuit for the case of isotropic distribution of slopes.

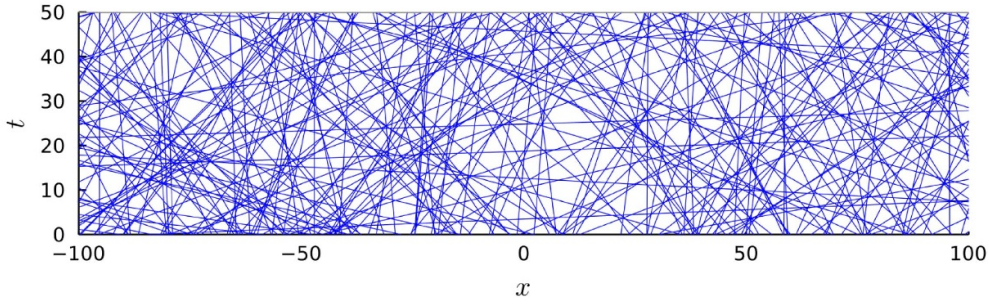

(d) Zoom out of the isotropic case.

Figure 2. Example of the two types of random mikado geometries studied.

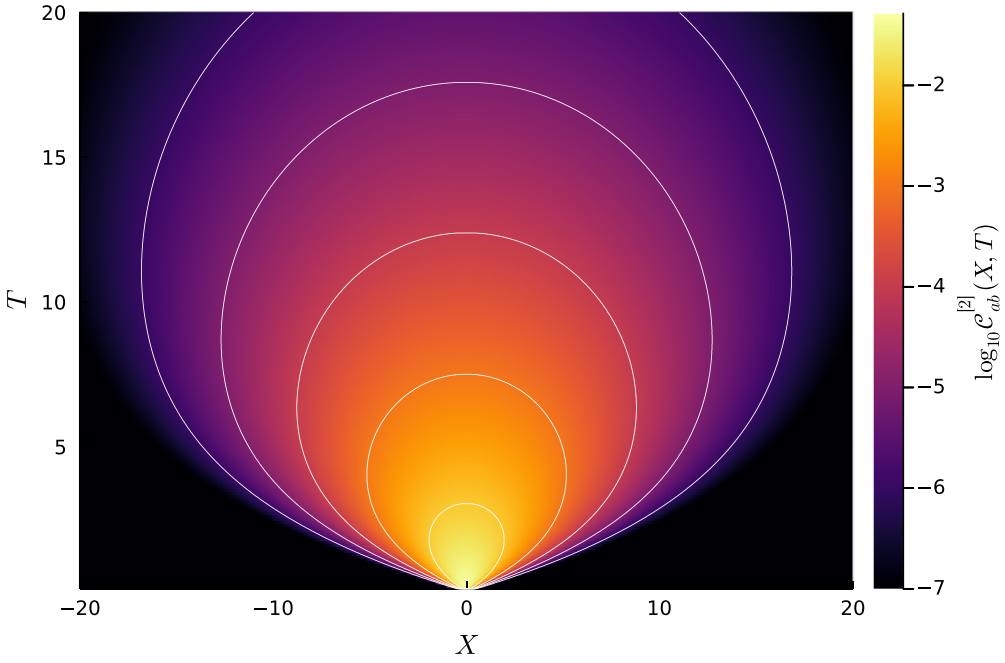

(a) Heatmap for the thermal case Eq. (27).

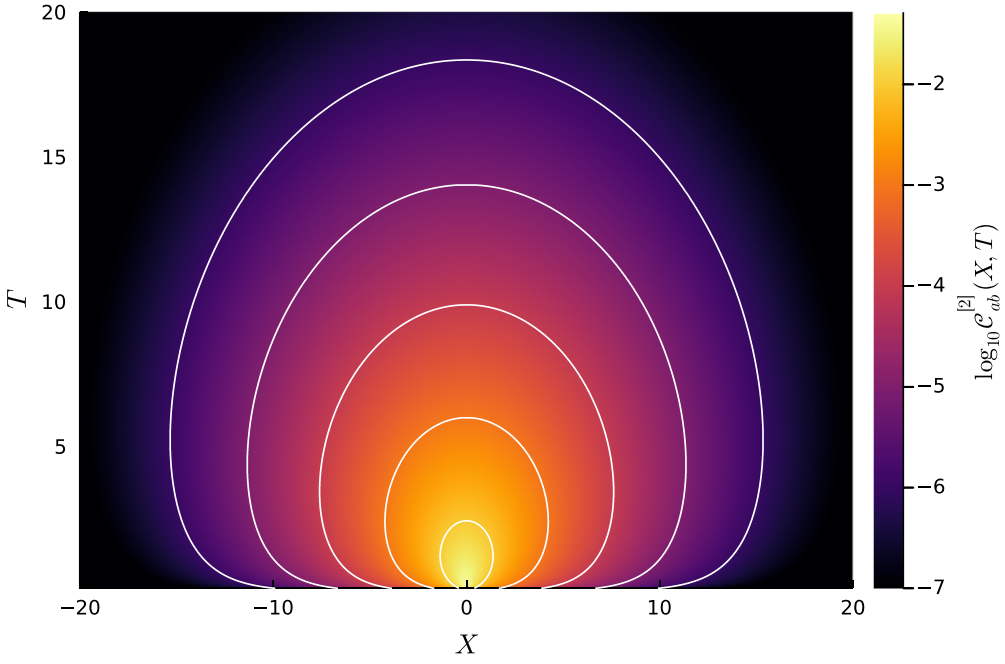

(b) Heatmap for the isotropic case Eq. (28)

Figure 3. Heatmaps of the fluctuation of the correlation functions with $J = \pi/4 - 1/2$ in log-scale, equation (26). The value of the variance of the correlation function are constant along the iso-contours drawn in white. We note that we took a cutoff for the minimum values shown at $\log_{10} \mathcal{C}^{[2]}_{ab}(X,T) = -7$.

5. Discussion

We proposed and explored random dual unitary circuits in random geometries. We studied two settings of the so-called mikado random geometries, one with a *preferred* space-time direction and the other with a *random* isotropic space-time. The first one can be physically motivated in terms of a thermalised ideal gas of identical classical point particles carrying quantum qubit degrees of freedom, which experience dual unitary scattering. The second one is a curious example of a euclidean space-time with equivalent unitary-quantum dynamics in a continuum set of directionalities. In both cases we have shown that, while the average local correlator vanishes due to randomness of the local gates, the variance of the correlator can be computed explicitly in terms of a simple rank-one transfer matrix. Computation of higher moments of the correlator involves a nontrivial Weingarten calculus and shall be left for future work.

Unitary dynamics in a continuum set of space-time directions found here should be contrasted with a pair of unitary directions in regular brickwork dual unitary circuits [2] or a triple of unitary space-time directions in the so-called tri-unitary circuits [13].

While this work addressed the simplest problem of computation of local correlations in mikado dual unitary circuits, there are several immediate pending questions for future explorations. For example, it would be interesting to compute entanglement dynamics, both for states and operators, study perturbed non-dual-unitary defects, or even attempt to extend the concepts of dual unitaries on random geometries to higher dimensions (in analogy to recent study [18]).

Last, but not least, one may wonder if an extension of random circuit geometry to arbitrary (non-mikado) graphs with degree 4 (i.e. *random 4-regular graphs*) would be feasible. Perhaps one can find a meaningful ensemble of planar random 4-regular graphs for this purpose. Clearly, in such cases, space-time paths which carry quantum information are no-longer straight lines, and interesting physical effects may occur when such paths can form self-intersections, or loops.

Data availability statement

All data that support the findings of this study are included within the article (and any supplementary files).

Acknowledgments

We thank Bruno Bertini, Felix Fritzsch and Pavel Kos for fruitful discussions. This research has received funding from the European Union's Horizon 2020 research and innovation programme under the Marie Skłodowska-Curie Grant Agreement No. 955479, and under ERC Advanced Grant 694544–OMNES, as well as from Slovenian Research agency (ARRS) under Programme P1-0402.

ORCID iDs

Yusuf Kasim https://orcid.org/0000-0003-1843-8716
Tomaž Prosen https://orcid.org/0000-0001-9979-6253

References

[1] Arute F *et al* 2019 *Nature* **574** 505–10
[2] Bertini B, Kos P and Prosen T 2019 *Phys. Rev. Lett.* **123** 210601
[3] Claeys P W and Lamacraft A 2020 *Phys. Rev. Res.* **2** 033032
[4] Claeys P W and Lamacraft A 2021 *Phys. Rev. Lett.* **126** 100603
[5] Rather S A, Aravinda S and Lakshminarayan A 2020 *Phys. Rev. Lett.* **125** 070501
[6] Aravinda S, Rather S A and Lakshminarayan A 2021 *Phys. Rev. Res.* **3** 043034
[7] Prosen T 2021 *Chaos* **31** 093101
[8] Piroli L, Bertini B, Cirac J I and Prosen T 2020 *Phys. Rev.* B **101** 094304
[9] Bertini B, Kos P and Prosen T 2018 *Phys. Rev. Lett.* **121** 264101
[10] Bertini B, Kos P and Prosen T 2021 *Commun. Math. Phys.* **387** 597–620
[11] Bertini B, Kos P and Prosen T 2020 *SciPost Phys.* **8** 67
[12] Kos P, Bertini B and Prosen T 2021 *Phys. Rev.* X **11** 011022
[13] Jonay C, Khemani V and Ippoliti M 2021 *Phys. Rev. Res.* **3** 043046
[14] Moca C P, Kormos M and Zaránd G 2017 *Phys. Rev. Lett.* **119** 100603
[15] Bañuls M C, Hastings M B, Verstraete F and Cirac J I 2009 *Phys. Rev. Lett.* **102** 240603
[16] Weingarten D 1978 *J. Math. Phys.* **19** 999–1001
[17] Collins B 2003 *Int. Math. Res. Not.* **2003** 953–82
[18] Milbradt R, Scheller L, Aßmus C and Mendl C B 2022 Ternary unitary quantum lattice models and circuits in $2+1$ dimensions arXiv:2206.01499